

Measuring the leading hadronic contribution to the muon g-2 via the μ -e elastic scattering

Umberto Marconi^{1,a} and Fulvio Piccinini^{2,b}

¹INFN Sezione di Bologna, Via Irnerio, 46 - 40126 Bologna (BO) Italy.

²INFN Sezione di Pavia, Via Agostino Bassi, 6 - 27100 Pavia (PV) Italy.

Abstract. The precision measurement of the anomalous magnetic moment $g-2$ of the muon presently exhibits a 3.5σ deviation between theory and experiments. In the next few years the anomalous magnetic moment will be measured to higher precisions at Fermilab and J-PARC. The theoretical prediction can be improved by reducing the uncertainty on the leading hadronic correction a_μ^{HLO} to the $g-2$. Here we present a novel approach to determine a_μ^{HLO} with space-like data, by means of precise measurement of the hadronic shift of the effective electromagnetic coupling α exploiting the elastic scattering of 150 GeV muons (currently available at CERN North area) on atomic electrons of a low-Z target. The direct measurement of a_μ^{HLO} in the space-like region will provide a new independent determination competitive with the time-like dispersive approach, and will consolidate the theoretical prediction of the muon $g-2$ in the Standard Model. It will allow therefore a firmer interpretation of the measurements of the future muon $g-2$ experiments at Fermilab and J-PARC

1 Introduction

The discrepancy between the experimental value of the muon anomalous magnetic moment $a_\mu = (g-2)/2$ and the Standard Model (SM) prediction, $\Delta a_\mu \sim (28 \pm 8) \times 10^{-10}$ is a long standing issue in particle physics [1, 2]. The current accuracy of the SM predictions, $\sim 5 \times 10^{-10}$, are limited by strong interaction effects, at the low energy scale implied. However by using analyticity and unitarity, it was shown [3] that the leading-order (LO) hadronic contribution to the muon $g-2$, a_μ^{HLO} , can be computed via a dispersion integral of the hadron production cross section in e^+e^- annihilation at low-energy. The present error on a_μ^{HLO} , $\sim 4 \times 10^{-10}$ or slightly better, with a relative accuracy of 0.6%, constitutes the main uncertainty of the SM prediction [4]. Alternative evaluations of a_μ^{HLO} can be obtained with QCD lattice calculations [5]. The current lattice QCD results are not yet competitive with the dispersive approach via time-like data, with errors that are expected to decrease significantly in the next few years [6]. The $O(\alpha^3)$ hadronic light-by-light contribution, a_μ^{HLbL} , which has the second largest error in the theoretical evaluation, contributing with an uncertainty of $(2.5-4) \times 10^{-10}$, cannot at present be determined from data and its calculation relies on the use of specific models [7–10].

The error achieved by the BNL E821 experiment [11], $\delta a_\mu^{\text{Exp}} = 6.3 \times 10^{-10}$, corresponding to 0.54 ppm, is dominated by the available statistics. New experiments at Fermilab and J-PARC, aiming at measuring the muon $g-2$ to a

precision of 1.6×10^{-10} (0.14 ppm), are in preparation [12–15].

Together with the experimental plans, an improvement on the value of the LO hadronic contribution is highly desirable. The proposal described here is to determine a_μ^{HLO} from a measurement of the effective electromagnetic coupling α in the space-like region, where the vacuum polarization is expected to be a smooth function of the squared momentum transfer. In this approach the hadronic contribution to the running of α can be measured by means of the t -channel $\mu - e$ elastic scattering process, from which a_μ^{HLO} can be determined directly [17]¹.

2 Measuring the Hadronic Leading contribution with space-like data.

For the calculation of the hadronic leading contribution a_μ^{HLO} with the t -channel approach an alternative formula to the dispersion integral [3, 21] can be exploited [18, 22], namely:

$$a_\mu^{\text{HLO}} = \frac{\alpha}{\pi} \int_0^1 dx (1-x) \Delta\alpha_{\text{had}}[t(x)], \quad (1)$$

where $\Delta\alpha_{\text{had}}(t)$ is the hadronic contribution to the running of the fine-structure constant, evaluated at

$$t(x) = \frac{x^2 m_\mu^2}{x-1} < 0, \quad (2)$$

¹The method has been originally proposed [18] by using Bhabha scattering data. A method to determine the running of α by using small-angle Bhabha scattering was proposed in [19] and applied to LEP data in [20].

^ae-mail: umberto.marconi@bo.infn.it

^be-mail: fulvio.piccinini@pv.infn.it

that is the space-like (negative) squared four-momentum transfer of the process. In contrast with the dispersive integral, the integrand of Eq. (1) is a smooth function and free of resonance poles. Fig. 1 (left) shows $\Delta\alpha_{\text{had}}$, and for comparison $\Delta\alpha_{\text{lep}}$, as a function of the variables x and t . The range $x \in (0, 1)$ corresponds to $t \in (-\infty, 0)$, with $x = 0$ for $t = 0$. The expected integrand of Eq. (1), calculated with the routine `hadr5n12` [23], which uses time-like hadroproduction data and perturbative QCD, is plotted in Fig. 1 (right). The peak of the integrand occurs at $x_{\text{peak}} \simeq 0.914$ (corresponding to $t_{\text{peak}} \simeq -0.108 \text{ GeV}^2$) and $\Delta\alpha_{\text{had}}(t_{\text{peak}}) \simeq 7.86 \times 10^{-4}$ (see Fig. 1 (right)).

We propose to use Eq. (1) to determine a_{μ}^{HLO} by measuring the running of α using the CERN muon beam of energy $E_{\mu} = 150 \text{ GeV}$, colliding on electron at rest of a fixed target. This technique is similar to the one used for the measurement of the pion form factor, as described in [24].

It looks very appealing for the following reasons:

- It is a t -channel process, making the dependence on t of the differential cross section proportional to $|\alpha(t)/\alpha(0)|^2$:

$$\frac{d\sigma}{dt} = \frac{d\sigma_0}{dt} \left| \frac{\alpha(t)}{\alpha(0)} \right|^2, \quad (3)$$

where $d\sigma_0/dt$ is the effective Born cross section, including virtual and soft photons, analogously to Ref. [25], where small-angle Bhabha scattering at high energy was considered. The vacuum polarization effect, in the leading photon t -channel exchange, is incorporated in the running of α and gives rise to the factor $|\alpha(t)/\alpha(0)|^2$.

- Given the incoming muon energy E_{μ} the t variable is related to the energy of the scattered electron E'_e or its angle θ_e through:

$$t = (p_{\mu} - p'_{\mu})^2 = (p_e - p'_e)^2 = 2m_e^2 - 2m_e E'_e, \quad (4)$$

$$s = (p'_{\mu} + p'_e)^2 = (p_{\mu} + p_e)^2 = m_{\mu}^2 + m_e^2 + 2m_e E_{\mu}, \quad (5)$$

$$E'_e = m_e \frac{1 + r^2 \cos^2 \theta_e}{1 - r^2 \cos^2 \theta_e}, \quad \theta_e = \arccos \left(\frac{1}{r} \sqrt{\frac{E'_e - m_e}{E'_e + m_e}} \right), \quad (6)$$

where the angle θ_e spans the range (0–31.85) mrad for the electron energy E'_e in the range (1–139.8) GeV.

- For $E_{\mu} = 150 \text{ GeV}$, it turns out that $s \simeq 0.164 \text{ GeV}^2$ and $-0.143 \text{ GeV}^2 < t < 0 \text{ GeV}^2$. It implies that the region of x extends up to 0.93, while the peak of the integrand function of Eq. (1) is at $x_{\text{peak}} = 0.914$, corresponding to an electron scattering angle of 1.5 mrad, as visible in Fig. 1 (right).
- The angles of the scattered electron and muon are correlated as shown in the Fig. 2, drawn for incoming muon energy of 150 GeV. This constraint is extremely important to select elastic scattering events, rejecting background events from radiative or inelastic processes and to minimize systematic effects in the determination of t . Note that for scattering angles of (2–3) mrad there is an ambiguity between the outgoing electron and muon, as their angles and momenta are similar, to be resolved by means of μ/e discrimination.

- The boosted kinematics allows the same detector to cover the whole acceptance. Many systematic errors, *e.g.* on the efficiency, will cancel out (at least at first order) in the relative ratios of event counts in the high and low q^2 regions (signal and normalization regions).

Assuming to use a muon beam of 150 GeV with an average intensity of $\sim 1.3 \times 10^7$ muon/s, with a running time of 2×10^7 s/yr, and using 30 experimental points in x (supplemented with large $|t|$ contributions that can be derived from pQCD), we estimate the statistical sensitivity of this experiment on the value of a_{μ}^{HLO} to be $\sim 0.3\%$. Such a beam is available at the CERN North Area.

3 Detection technique

The CERN muon beam M2 presents ideal characteristics to perform for the measurement. The beam intensity, of more than 10^7 muon/s, can provide the required event yield and its time structure allows to tag the incident muon. The target must be of low- Z material, and the whole target thick such (order of 60 cm) to get enough electron scattering centres. The low- Z requirement is in order to minimize multiple scattering and to have high radiation length. The idea is them to use a segmented target of 1 cm thin layers, distributed in 60 identical modules. Each detection module has the size of 50 cm and consists of a thin target of Be (or C), coupled to three Si planes for tracking (no magnetic field applied). Fig. 3 shows the basic layout. Downstream the tracking modules, as particle identifiers, we plan to use a calorimeter for the electrons. They are required in order to solve the muon-electron ambiguity for electron scattering angles around (2–3) mrad *cf.* Fig. 2. The preliminary studies of such an apparatus, performed by using GEANT4, indicate an angular resolution of ~ 0.02 mrad for the outgoing particles. The detector acceptance covers both the region of the signal, with the electron emitted at extremely forward angles and high energies, and the normalization region, where the electron has much lower energy (around 1 GeV) and an emission angle of some tens of mrad. Due to the boosted kinematics of the collisions, the detector covers most of the acceptance, and let all the scattering angles in the laboratory system to be accessed by a single detector element.

4 Considerations on systematic uncertainties

Significant contributions of the hadronic vacuum polarization to the $\mu e \rightarrow \mu e$ differential cross section are essentially restricted to electron scattering angles below 10 mrad, corresponding to electron energies above 10 GeV. The net effect of these contributions is to increase the cross section by a few per mille: a precise determination of a_{μ}^{HLO} requires not only high statistics, but also a high level of control of systematic uncertainties, both on the theory as well as the experimental side, as the final goal of the experiment is equivalent to a determination of the differential cross section with ~ 10 ppm systematic uncertainty at the peak of the integrand function (*cf.* Fig. 1).

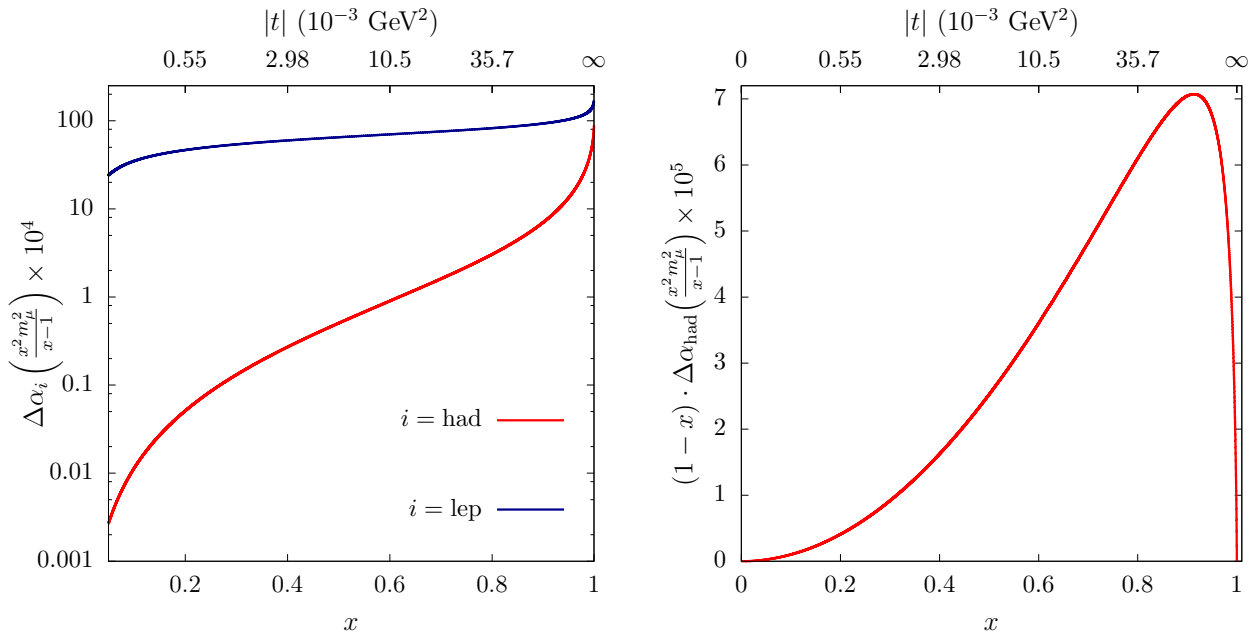


Figure 1. Left: $\Delta\alpha_{\text{had}}[t(x)] \times 10^4$ (red) and, for comparison, $\Delta\alpha_{\text{lep}}[t(x)] \times 10^4$ (blue), as a function of x and t (upper scale). Right: the integrand $(1-x)\Delta\alpha_{\text{had}}[t(x)] \times 10^5$ as a function of x and t . The peak value is at $x_{\text{peak}} \approx 0.914$, corresponding to $t_{\text{peak}} \approx -0.108 \text{ GeV}^2$.

4.1 Experimental systematic uncertainties

A crucial requirement on the experimental side is to keep the efficiency highly uniform over the entire q^2 range, including the normalization region, and over all the detector components. This motivates the choice of a purely angular measurement: an acceptance of tens of mrad can be covered with a single sensor of modern silicon detectors, positioned at a distance of $\sim 1 \text{ m}$ from the target. It has to be stressed that particle identification (electromagnetic calorimeter and muon filter) is necessary to solve the electron-muon ambiguity in the region below 5 mrad. The wrong assignment probability can be measured with the data by using the rate of muon-muon and electron-electron events.

Another requirement for reaching very high accuracy is to measure all the relevant contributions to systematic uncertainties from the data themselves. An important effect, which distinguishes the normalization from the signal region, is multiple scattering, as the electron energy in the normalization region is as low as 1 GeV. Multiple scattering breaks the muon-electron two-body angular correlation, moving events out of the kinematic line in the 2D plot of Fig. 2. In addition, multiple scattering in general causes acoplanarity, while two-body events are planar, within the resolution. These facts allow effects to be modelled and measured by using data. An additional handle on multiple scattering could be the inclusion of a thin layer in the apparatus, made of the same material as the main target modules. This possibility will be studied in detail with simulation.

In high-precision experiments several systematic effects can be explored within the experiment itself. In this respect the proposed modularity of the apparatus will

help. A test with a single module could provide a proof-of-concept of the proposed method.

4.2 Theoretical systematic uncertainties

Since the final goal of the experiment is a high precision measurement of a differential cross section, the latter has to be calculated with all the radiative corrections relevant at the precision scale of 0.01%. Such an accuracy has never been achieved in a collision experiment. The most precise experiments has been conducted at leptonic colliders such as LEP and flavour factories [26], where the theoretical precision at the level of 0.1% (or even better, as for small angle Bhabha scattering at LEP) was achieved. Previous quantitative considerations of Eq. (3) and Eq. (6) are based on the QED Leading Order (LO) expression of the differential cross section for $\mu e \rightarrow \mu e$

$$\frac{d\sigma}{dt} = \frac{4\pi\alpha^2}{\lambda(s, m_\mu^2, m_e^2)} \left[\frac{(s - m_\mu^2 - m_e^2)^2}{t^2} + \frac{s}{t} + \frac{1}{2} \right]. \quad (7)$$

The effect of running of α introduced in Eq. (3) is obtained by resumming to all orders the gauge invariant subset of fermionic corrections at $\mathcal{O}(\alpha)$. At the same next-to-leading order (NLO), the class of QED corrections due to the insertion of a photon line, virtual and real, contribute. These corrections are known in the literature for μe scattering [27] but need to be implemented in a Monte Carlo event generator [28] tailored to simulate the present energy and kinematics conditions, in order to design the optimal detector configuration and the event selection for data analysis. The typical theoretical uncertainty of a QED NLO calculation is of the order of 1%. The techniques to match NLO fixed order calculation with all-orders resummed calculations of leading logarithmic contributions

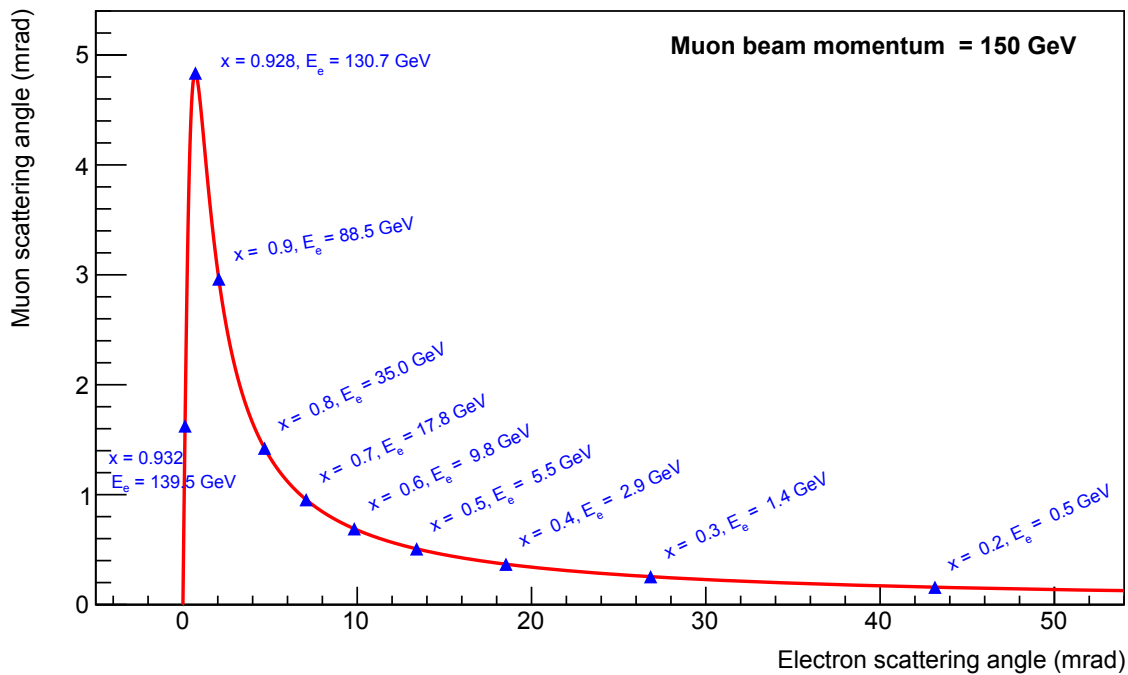


Figure 2. The relation between the muon and electron scattering angles for 150 GeV incident muon beam momentum. Blue triangles indicate reference values of the Feynman's x and electron energy.

are well known in QED [29] and allow to reach accuracies at the 0.1% level. In order to go beyond this limit, the NNLO QED corrections are required. A first step in this direction has been undertaken through the evaluation of the planar master integrals related to the two-loop photonic box diagrams of the virtual QED corrections to the $\mu e \rightarrow \mu e$ process, in the approximation of massless electron [30]. Once the calculation of the non-planar contributions will be carried out, all the building blocks for the complete photonic QED NNLO calculation will be available. At two loop level, also fermionic one-loop insertions on top of QED NLO diagrams have to be evaluated. Such contributions have already been evaluated for Bhabha scattering [31]. The virtual contribution involves also the effect of hadronic vacuum polarization, which requires a dedicated study [32]. The real pair emission is also particularly important since one of the leptons of the additional pair can produce by itself a signal track. The evaluation of such contributions requires, therefore, a detailed Monte Carlo simulation with realistic geometric acceptance. Such kind of studies have been performed already for LEP physics [33].

Another class of contributions is given by the Z^0 tree-level exchange diagram and the full NLO corrections in the electroweak standard model. Even if they are expected to be small, it is worth to quantify their size. These corrections have been calculated in the literature [34]. A complete evaluation and Monte Carlo implementation is in progress [28].

5 Conclusions

The experiment MUonE presented to determine the leading hadronic contribution to the muon $g-2$, by scattering high-energy muons on atomic electrons of a low- Z target through the process $\mu e \rightarrow \mu e$, is primarily based on a precise measurement of the scattering angles of the two outgoing particles as the q^2 of the muon-electron interaction can be directly determined by the electron (or muon) scattering angle. An advantage of the muon beam is the possibility of employing a modular apparatus, with the target subdivided in subsequent layers. A low- Z solid target is preferred in order to provide the required event rate, limiting at the same time the effect of multiple scattering as well as of other types of muon interactions (pair production, bremsstrahlung and nuclear interactions). The normalization of the cross section is provided by the very same $\mu e \rightarrow \mu e$ process in the low- q^2 region, where the effect of the hadronic corrections on $\alpha(t)$ is negligible. Such a simple and robust technique has the potential to keep systematic effects under control, aiming at reaching a systematic uncertainty of the same order as the statistical one. For this purpose a preliminary detector layout has been described. On the theoretical side, the radiative corrections at NNLO accuracy have to be considered in full detail and a Monte Carlo event generator able to match fixed order NNLO predictions with resummation given by the Parton Shower technique is needed. By considering a beam of 150 GeV muons with an average intensity of $\sim 1.3 \times 10^7$ muon/s, currently available at the CERN North Area, a statistical uncertainty of $\sim 0.3\%$ can be achieved on a_μ^{HLO} in

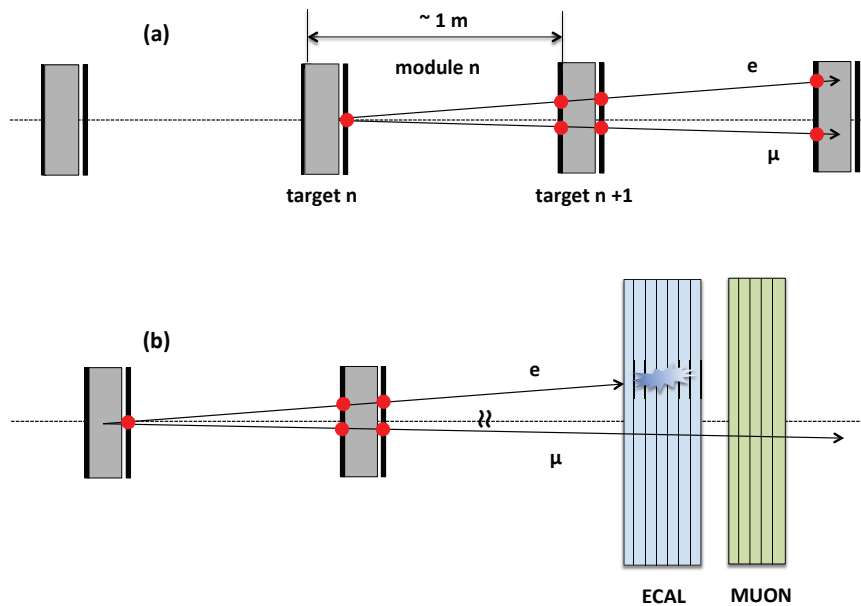


Figure 3. Scheme of a possible detector layout. (a) The detector is a modular system. Each module consists of a low-Z target (Be or C) and three silicon tracking stations within the distance of 50 cm. (b) To perform the μ -e discrimination in the case of small scattering angles (with both θ_μ and θ_e below 5 mrad) the detector is equipped with an electromagnetic calorimeter and a muon detector.

two years of data taking. A test performed using a single detector module, exploiting the muon beam facility, could provide a validation of the proposed method.

Acknowledgements

We thank G. Abbiendi, C.M. Carloni Calame, C. Matteuzzi, G. Montagna, O. Nicosini, M. Passera, R. Tenchini, L. Trentadue and G. Venanzoni for fruitful and pleasant collaboration. We thank the organizers of the FCCP2017 Workshop for their kind invitation.

References

- [1] T. Blum, A. Denig, I. Logashenko, E. de Rafael, B. Lee Roberts, T. Teubner and G. Venanzoni, arXiv:1311.2198 [hep-ph].
- [2] F. Jegerlehner, EPJ Web Conf. **118** (2016) 01016.
- [3] C. Bouchiat, L. Michel, J. Phys. Radium **22** (1961) 121;
 L. Durand, Phys. Rev. **128** (1962) 441 [Erratum-ibid. **129** (1963) 2835];
 M. Gourdin, E. De Rafael, Nucl. Phys. B **10** (1969) 667.
- [4] D. Nomura, these proceedings.
- [5] C. Aubin, T. Blum, Phys. Rev. D **75** (2007) 114502;
 P. Boyle, L. Del Debbio, E. Kerrane, J. Zanotti, Phys. Rev. D **85** (2012) 074504;
 X. Feng, K. Jansen, M. Petschlies, D.B. Renner, Phys. Rev. Lett. **107** (2011) 081802;
 M. Della Morte, B. Jager, A. Juttner, H. Wittig, JHEP **1203** (2012) 055;
 T. Blum *et al.*, Phys. Rev. Lett. **116** (2016) no.23, 232002;
 B. Chakraborty, C. T. H. Davies, P. G. de Oliveira, J. Koponen and G. P. Lepage, arXiv:1601.03071 [hep-lat].
- [6] T. Blum, M. Hayakawa, T. Izubuchi, PoS LATTICE **2012** (2012) 022;
 B. Chakraborty, C. Lehner, R. Van de Water, talks at ICHEP 2016, <https://indico.cern.ch/event/432527/contributions/speakers>
- [7] M. Knecht, A. Nyffeler, Phys. Rev. D **65** (2002) 073034;
 K. Melnikov, A. Vainshtein, Phys. Rev. D **70** (2004) 113006;
 J. Prades, E. de Rafael, A. Vainshtein, arXiv:0901.0306 [hep-ph].
 F. Jegerlehner, A. Nyffeler, The Muon $g-2$, Phys. Rept. **477** (2009) 1;
 A. Nyffeler, Phys. Rev. D **79** (2009) 073012.
- [8] F. Jegerlehner, A. Nyffeler, Phys. Rept. **477** (2009) 1.
- [9] C. Lehner, these proceedings.
- [10] A. Nyffeler, these proceedings.
- [11] G. W. Bennett *et al.* (The $g-2$ Collaboration), Phys. Rev. **D73** (2006) 072003.

- [12] J. Grange *et al.* [Muon $g-2$ Collaboration], arXiv:1501.06858 [physics.ins-det].
- [13] N. Saito [J-PARC $g-2$ /EDM Collaboration], AIP Conf. Proc. **1467** (2012) 45.
- [14] T. Gorringer, these proceedings.
- [15] G. Marshall, these proceedings.
- [16] M. Davier, A. Hoecker, B. Malaescu and Z. Zhang, Eur. Phys. J. **C71** (2011) 1515, Erratum-ibid. **C72** (2012) 1874.
- [17] G. Abbiendi, C. M. Carloni Calame, U. Marconi, C. Matteuzzi, G. Montagna, O. Nicosini, M. Passera, F. Piccinini, R. Tenchini, L. Trentadue and G. Venanzoni, Eur. Phys. J. C (2017) 77 139.
- [18] C. M. Carloni Calame, M. Passera, L. Trentadue and G. Venanzoni, Phys. Lett. B **746** (2015) 325
- [19] A.B. Arbuzov, D. Haidt, C. Matteuzzi, M. Paganoni and L. Trentadue, Eur. Phys. J. C **34** (2004) 267.
- [20] G. Abbiendi *et al.* [OPAL Collaboration], Eur. Phys. J. C **45** (2006) 1.
- [21] F. Jegerlehner, Springer Tracts Mod. Phys. **226**, 2008.
- [22] B.E. Lautrup, A. Peterman, E. de Rafael, Phys. Rept. **3** (1972) 193.
- [23] S. Eidelman and F. Jegerlehner, Z. Phys. C **67** (1995) 585;
F. Jegerlehner, Nucl. Phys. Proc. Suppl. **181-182** (2008) 135
- [24] S. R. Amendolia *et al.*, Phys. Lett. B **146** (1984) 116;
S. R. Amendolia *et al.* [NA7 Collaboration], Nucl. Phys. B **277** (1986) 168.
- [25] A.B. Arbuzov, V.S. Fadin, E.A. Kuraev, L.N. Lipatov, N.P. Merenkov, L. Trentadue, Nucl. Phys. B **485** (1997) 457;
- [26] B.F.L. Ward *et al.*, Phys. Lett. **B450** (1999) 262;
S. Actis *et al.*, Eur. Phys. J. C66 (2010) 585-686.
- [27] K.E. Eriksson, Nuovo Cimento **19** (1961) 1029;
A.I. Nikishov, Sov. Phys. JETP (1961) 1929;
K.E. Eriksson, B. Larsson and G.A. Rinander, Nuovo Cimento **30** (1963) 1434; P. Van Nieuwenhuizen, Nucl. Phys. B **28** (1971) 429; T. V. Kukhto, N. M. Shumeiko and S. I. Timoshin, J. Phys. G **13** (1987) 725; D. Y. Bardin and L. Kalinovskaya, DESY-97-230, hep-ph/9712310; N. Kaiser, J. Phys. G **37** (2010) 115005.
- [28] M. Alacevich *et al.*, work in progress.
- [29] G. Balossini *et al.*, Nucl.Phys. B758 (2006) 227-253.
- [30] P. Mastrolia *et al.*, JHEP 1711 (2017) 198.
- [31] C.M. Carloni Calame *et al.*, JHEP 1107 (2011) 126;
Nucl. Phys. Proc. Suppl. 225-227 (2012) 293
- [32] M. Fael and M. Passera, work in progress.
- [33] G. Montagna *et al.*, Nucl. Phys. **B547** (1999) 39;
Phys. Lett. **B459** (1999) 649.
- [34] E. Derman and W.J. Marciano, Ann. Phys. **121** (1979) 147; G. D'Ambrosio, Lett. Nuovo Cim. **38** (1983) 593; J.C. Montero, V. Pleitez and M.C. Rodriguez, Phys. Rev. **D58** (1998) 097505.